Analyzing Finger-Movement Trajectories with Stochastic Differential Equations (SDEs)

Valerie Morash[1] and David Brillinger[2]

Abstract— **Fingertip positions can be conceptualized as Brownian particles within a force field. Using stochastic differential equations (SDEs) the force field and its associated potential function can be formally related to observed fingertip positions. Using observed fingertip positions the force field can then be "solved." This provides a means of describing, comparing, and simulating finger-movement trajectories without formulating the kinematics of the hand. Through discretization of SDEs, the resulting mathematical forms are merely regression equations, which can be solved using familiar mathematical tools such as ordinary least squares and maximum likelihood estimation. Experimental "effects" are specified in the force-field part of the regression, and the Brownian perturbances as the random error of the regression. Using SDEs to specify potential functions can support haptic scientists performing exploratory data analysis, wishing to summarize finger-movement trajectories, compare and test differences in finger-movement trajectories between participants, groups of participants, or experimental conditions, and simulate/predict finger-movement trajectories.**

I. MOTIVATION

This paper presents a framework for analyzing finger-movement trajectories as Brownian particles using stochastic differential equations (SDEs). SDEs have have been successfully used to model other movement trajectories, such as animal movements [1], [2], [3], but this has been done using approximations that do not include terms for momentum. Typical finger-movement trajectories recorded during haptic experiments are finely sampled so that time-adjacent positions typically describe a single direction of movement, i.e., movement in a straight line, can be modeled as momentum in a Brownian particle. Therefore, the current paper's contributions include extending the existing SDE framework to include momentum, and illustrating how to this framework can be used to model finger-movement trajectories.

Critical to this approach is conceptualizing fingertip position as a Brownian particle. Besides a random component, the finger's movements are affected by its environment, typically the stimulus being explored. This is achieved by formulating a force field associated with the stimulus. This force field pushes the finger towards points of attraction, e.g., useful stimulus features, and away from points of repulsion, e.g., the stimulus border or features not pertinent to the task. The force field is generated through a potential function, with areas of high potential that are repulsive, like a hill, and areas of low potential that are attractive, like a valley. The potential function and force field are formally related through partial derivatives, and their parameters are estimated using *linear regression* with the observed finger positions.

When applying this approach, the goal will often be to solve the potential function from observed finger-movement trajectories. The potential function of a particular stimulus may be of interest, and/or how the potential function is affected by experimental groups/conditions. A particular experiment will likely compare the potential functions for different designs of stimuli, groups of participants, or other experimentally manipulated conditions. Another use of this approach is to simulate finger-movement trajectories. Observations of finger movements over a set of stimuli can be used to generate predicted trajectories over novel stimuli.

The current paper presents the mathematical background/derivation of the SDE approach, followed by an illustrative example of analyzing finger-trajectory data. The mathematical background is covered in detail, with the goal of being a comprehensive introduction accessible to both haptic psychologists and engineers.

II. MATHEMATICAL BACKGROUND

There are two mathematical descriptions of Brownian motion, the constant random motion of particles. Einstein's 1905 derivation of Brownian motion from the molecular-kinetic theory of heat [4] resulted in a partial differential equation, the simplest case of a class of equations now known as the Fokker-Planck equations, which specified the time evolution of the probability density of a Brownian particle. In 1908 Paul Langevin applied Newton's second law to the motions of a representative Brownian particle. Both Einstein's and Langevin's approaches have been used to derive similar results, while the latter is viewed as slightly more general and correct, simpler, and with immediate connection to Newtonian dynamics [5], [6]. Langevin's equation is also notable as the first example of a stochastic differential equation [5], and serves as the basis for the current work.

A. The Langevin Equation

Starting with Newton's second law, Langevin wrote the position $\mathbf{r}(t) = (x(t), y(t))^{\mathrm{T}}$ of a Brownian particle with mass m at time t, assuming $d\mathbf{r}(t)/dt = \mathbf{v}(t)$ and $d^2\mathbf{r}(t)/dt^2 = d\mathbf{v}(t)/dt$ exist, as

$$\underbrace{m\frac{d^2\mathbf{r}(t)}{dt^2}}_{\text{force}} = \underbrace{-b\frac{d\mathbf{r}(t)}{dt}}_{\text{friction}} + \underbrace{\boldsymbol{\eta}(t)}_{\text{random}} \quad (1)$$

where b is a friction constant, governed by Stokes's law, and $\boldsymbol{\eta}(t)$ is a bivariate Gaussian random variable. This expresses

[1]Valerie Morash is with the Smith-Kettlewell Eye Research Institute, 2318 Fillmore Street, San Francisco, CA 94115, USA val@ski.org

[2]David Brillinger is with the Statistics Department, University of California, Berkeley, CA 94720-3860, USA. brill@stat.berkeley.edu

the force on the particle in two parts, a frictional force, $-b\mathbf{v}(t)$, and a fluctuating random force due to molecular collisions, $\boldsymbol{\eta}(t)$, [5], [7]. Langevin introduced the random "complementary force" to maintain the particle's agitation. Without the complementary force, the viscous resistance (frictional force) would stop [6]. The random force takes the form of a Wiener process, i.e., standard Brownian motion, which is the integral of Gaussian white noise [8], [7].

1) External Force Field: In the case that the particle is in an external force field, where the acceleration due to this force field is $K(\mathbf{r}(t), t)$, then the Langevin equation becomes,

$$\underbrace{m\frac{d^2\mathbf{r}(t)}{dt^2}}_{\text{force}} = \underbrace{K(\mathbf{r}(t), t)}_{\text{force field}} - \underbrace{b\frac{d\mathbf{r}(t)}{dt}}_{\text{friction}} + \underbrace{\frac{d\mathbf{B}(t)}{dt}}_{\text{random}} \tag{2}$$

where $\mathbf{B}(t)$ is a Wiener process with variance parameter $2b^2D$ [9, Eqs. 317-318], [7, eq. 10.1 & ch. 12].[1] Einstein was the first to derive $D = (kT)/b$, where k is the Boltzmann constant and T is absolute temperature.

2) Smoluchowski Approximation: Under the assumption that the coefficient of friction, $\beta = b/m$, is large, or equivalently mass, m, is small, the so-called Smoluchowski approximation to this equation is,

$$b\frac{d\mathbf{r}(t)}{dt} = K(\mathbf{r}(t), t) + \frac{d\mathbf{B}(t)}{dt} \tag{3}$$

where $\mathbf{B}$ is a Wiener process with variance parameter $2b^2D$ [7, pp. 58 & ch. 10]. Note that because momentum can only exist for a particle that has mass, the Smoluchowski approximation removes momentum from the Langevin equation. This is the approximation used in prior work on animal movements [1], [2], [3].

B. The Potential Function

In many applications, the force field, $K(\mathbf{r}(t), t)$, is taken to be a conservative force field, derived from a smooth real-valued potential function $H(\mathbf{r}(t), t)$,

$$K(\mathbf{r}(t), t) = -\nabla H(\mathbf{r}(t), t) = \boldsymbol{\mu}(\mathbf{r}(t), t) \tag{4}$$

where $\nabla = (\partial/\partial x, \partial/\partial y)^{\mathrm{T}}$ is the gradient operator [10, pp. 280], and the negative sign results from conservation of energy. The force-related acceleration $\boldsymbol{\mu}(\mathbf{r}(t), t) = (\mu_x(\mathbf{r}(t), t), \mu_y(\mathbf{r}(t), t))^{\mathrm{T}}$ is in many situations conceptualized as a drift parameter [11], [2], [3].

C. Relating the Potential Function to Data

In haptics research, the potential function will be used to examine how finger movements are affected by the stimulus. The potential function, $H(\mathbf{r}(t), t)$, and associated force field, $\boldsymbol{\mu}(\mathbf{r}(t), t)$, will be functions of the finger position, $\mathbf{r}(t)$, and important stimulus features taking the form of points, lines, or regions [3]. Frequently, the potential is a function of the shortest distance between the finger and a stimulus feature, i.e., $H(\mathbf{r}(t), t) = h(d(\mathbf{r}, t))$ for some function $h(\cdot)$ and $d(\mathbf{r}(t))$ being the shortest distance between the finger and feature [2].

A common scheme is one of attraction/repulsion, where $h(d(\mathbf{r}(t), t)) = \alpha(\mathbf{r}(t) - \mathbf{a})^2$, which is the Ornstein-Uhlenbeck (O-U) process, and describes attraction/repulsion to a point $\mathbf{a}$. This potential surface either takes the form of a repulsive hill ($\alpha < 0$) or an attractive valley ($\alpha > 0$), centered on point $\mathbf{a}$ with height proportional to the constant α. The steepness of the hill/valley can vary depending on the axis if the amplitude is a vector $\boldsymbol{\alpha} = (\alpha_x, \alpha_y)^{\mathrm{T}}$.

Several potential functions of this type, labeled $k = 1, \ldots, n$, can be incorporated linearly (Eq. 5), resulting in their combined force fields also combining linearly (Eq. 6).

$$H(\mathbf{r}(t), t) = h_1(d_1(\mathbf{r}(t)), t) + \cdots + h_n(d_n(\mathbf{r}, t)) \tag{5}$$

$$\boldsymbol{\mu}(\mathbf{r}(t), t) = -2(\mathbf{r}(t) - \mathbf{a}_1)h_1' - \cdots - 2(\mathbf{r}(t) - \mathbf{a}_n)h_n' \tag{6}$$

where $\mathbf{a}_k = (x_k, y_k)^{\mathrm{T}}$ is the location of the kth attraction or repulsion region, and h_k' is the partial derivative of h_k with respect to $d_k^2 = (x(t) - x_k)^2 + (y(t) - y_k)^2$ [2]. More generally, multiple potential functions of any form can be added linearly to create a composite potential function whose force fields also add linearly. This is particularly useful for creating a stimulus potential function that is formed by individual features' potential functions.

There are many parametric potential surfaces beyond O-U, including Gaussian, gravitational, and Zohdi shapes [12]; in addition to smooth non-parametric functions and high-degree polynomials [2], [3], [13]. It is important to note that when the potential function is a polynomial, the degree of the polynomial is arbitrary and is only chosen to provide a nonlinear shape. As such, interpretation comes from the overall shape of the potential function, and not from individual parameters [12].

D. Modeling: Discretization, Estimation, & Simulation

1) Discretization: The Langevin equation (Eq. 2) must be discretized to be applied to data discretely sampled in time. There are several numerical methods for discretizing differential equations. We use the Taylor series approximations for the time derivatives of position (velocity and acceleration). We will write $\Delta t_i = t_{i+1} - t_i = \Delta t$, $i = 1, \ldots, N$, specifying that the data were sampled at a constant rate.

The Euler method (first-order approximation) can be used to discretize the Smoluchowski approximation (Eq. 3), but a second-order expansion is necessary for the Langegvin equation (Eq. 2). It is straightforward to show that, using neighboring positions and second-order Taylor expansions, velocity and acceleration at time t can be expressed as,

$$\begin{aligned} \text{Velocity: } \mathbf{r}'(t_i) &\approx \frac{\mathbf{r}(t_{i+1}) - \mathbf{r}(t_{i-1})}{2\Delta t} \\ \text{Acceleration: } \mathbf{r}''(t_i) &\approx \frac{\mathbf{r}(t_{i-1}) - 2\mathbf{r}(t_i) + \mathbf{r}(t_{i+1})}{\Delta t^2} \end{aligned} \tag{7}$$

[1] This formula is alternatively often expressed with $\beta = b/m$ and $K = F/m$ for force F. Here we use K as the force field directly.

Then, the Langevin equation (Eq. 2) can be written as,

$$m\frac{\mathbf{r}(t_{i+1}) - 2\mathbf{r}(t_i) + \mathbf{r}(t_{i-1})}{\Delta t^2} = \boldsymbol{\mu}(\mathbf{r}(t_i), t_i) - b\frac{\mathbf{r}(t_{i+1}) - \mathbf{r}(t_{i-1})}{2\Delta t} + \boldsymbol{\Sigma}(\mathbf{r}(t_i), t_i)\mathbf{Z}(t_i)\Delta t^{-1/2} \quad (8)$$

where entries of $\mathbf{Z}(t_i)$ are independent standard normals. The random term is setup such that $\text{Cov}[\boldsymbol{\Sigma}(\mathbf{r}(t_i), t_i)\mathbf{Z}(t_i)\Delta t^{-1/2}] = \boldsymbol{\Sigma}(\mathbf{r}(t_i), t_i)$.

Note that in Eq. 8, Δt is a known constant and the positions, $\mathbf{r}(t_i) = (x_i, y_i)$, are observed. The goal is to estimate the parameters of μ_x, μ_y, b, and m, and possibly $\boldsymbol{\Sigma}$. These unknown parameters can be estimated using conventional schemes, such as maximum likelihood estimation (MLE).

2) Estimating the Langevin Parameters: For model estimation purposes, it is useful to re-write the Langevin discretization (Eq. 8) as an autoregressive model,

$$\mathbf{r}(t_{i+1}) = \left(\frac{2m}{\frac{1}{2}b\Delta t + m}\right)\mathbf{r}(t_i) + \left(\frac{\frac{1}{2}b\Delta t - m}{\frac{1}{2}b\Delta t + m}\right)\mathbf{r}(t_{i-1}) + \left(\frac{\Delta t^2}{\frac{1}{2}b\Delta t + m}\right)\boldsymbol{\mu}(\mathbf{r}(t_i), t_i) + \left(\frac{\Delta t^2}{\frac{1}{2}b\Delta t + m}\right)\boldsymbol{\Sigma}(\mathbf{r}(t_i), t_i)\mathbf{Z}(t_i)\Delta t^{-1/2} \quad (9)$$

The equivalent Smoluchowski approximation (Eq. 3) used in previous research is,

$$\mathbf{r}(t_{i+1}) = \mathbf{r}(t_i) + \frac{\Delta t}{b}\boldsymbol{\mu}(\mathbf{r}(t_i), t_i) + \frac{\Delta t}{b}\boldsymbol{\Sigma}(\mathbf{r}(t_i), t_i)\mathbf{Z}(t_i)\Delta t^{-1/2} \quad (10)$$

The autoregressive term in Eq. 9 is absent in Eq. 10. If γ_1 and γ_2 represent the coefficients in front of $\mathbf{r}(t_i)$ and $\mathbf{r}(t_{i-1})$ in Eq. 9, respectively, then solving for m and b in terms of γ_1 and γ_2 is under-constrained because $\gamma_1 + \gamma_2 = 1$. One may choose to not fix the variance of the stochastic term, and instead fix $b \equiv 1$, permitting the comparison of "momentum" in stochastic models based on mass, m, alone. Then, $\gamma_1 = \frac{2m}{\frac{1}{2}b\Delta t + m}$, $\gamma_2 = \frac{\frac{1}{2}b\Delta t - m}{\frac{1}{2}b\Delta t + m}$, and $m = \frac{\gamma_1 \Delta t}{2(\gamma_2 + 1)}$.

3) Simulation - Time Marching: The time marching simulation of the Smoluchowski approximation is straightforward using the Euler approximation, and can be used directly from Eq. 10. However, in the case of the Langevin equation, the second-order differential equation,

$$\mathbf{r}''(t) = -\frac{b}{m}\mathbf{r}'(t) - \frac{1}{m}\nabla H(\mathbf{r}(t), t) + \frac{1}{m}\boldsymbol{\eta}(t) \quad (11)$$

where $\mathbf{B}(t)$ is a two-dimensional Wiener process, for positions $\mathbf{r}(t) = (x(t), y(t))^{\mathrm{T}}$, and $\mathbf{W}'(t) = \boldsymbol{\eta}(t)$, must be rewritten as a first-order system for time marching. It is straightforward to rewrite the second-order differential equation for the Langevin equation as the following first-order differential system,

$$\mathbf{X}(t) = \begin{bmatrix} x_1(t) \\ x_2(t) \end{bmatrix} = \begin{bmatrix} \mathbf{r}(t) \\ m\mathbf{r}'(t) - w(t) \end{bmatrix}$$
$$\mathbf{X}'(t) = \begin{bmatrix} x_1'(t) \\ x_2'(t) \end{bmatrix} = \begin{bmatrix} \frac{1}{m}\Big(x_2(t) + w(t)\Big) \\ -\frac{b}{m}\Big(x_2(t) + w(t)\Big) - \nabla H(\mathbf{r}(t), t) \end{bmatrix} \quad (12)$$

Then a time-marching simulation can be performed using the Euler approximation,

$$\mathbf{X}(t_{i+1}) = \mathbf{X}(t_i) + \Delta t\mathbf{X}'(t_i) \quad (13)$$

E. Special Types of Random Walks

In addition to the Ornstein-Uhlenbeck process already described, the SDE framework can accommodate other special types of random walks. A *biased* random walk has a tendency to move in a particular direction, captured by the average drift velocity $\boldsymbol{\mu}$. For constant $\boldsymbol{\mu} = \mathbf{A}$, movement drifts in the direction of $\mathbf{A}$ [2].

A *correlated* random walk describes situations when the walker has a tendency, a.k.a, inertia, momentum, or persistence to keep walking in the current direction [14]. In this situation, the walker's position is no longer a Markov process, but its velocity is [15]. The presence of autoregressive terms (as in the Langevin Eq. 9 allows for correlation [12].

A random walk with a *barrier/boundary* is accomplished using a potential function that is nonzero only when $\mathbf{r}(t)$ is on or over the boundary, and increases with distance from the boundary [1].

III. ILLUSTRATIVE EXAMPLE

A. Methods

1) Participants: Three blind and three sighted individuals participated in this research. The blind participants used braille as their primary literacy medium (ages 22, 39, and 38 years old, two females). The three sighted participants were age-gender matches to the blind participants (ages 23, 39, and 36 years old, two females). The protocol was approved by the Smith-Kettlewell institutional review board, and informed consent was obtained from all participants prior to their participation.

2) Materials and Procedures: Fourteen stimuli were created on 9 by 9 in. thermoform sheets, each containing 3-5 symbols with random rotation and placement. Of the 14 stimuli, 7 contained only T symbols (height 0.3 in., width 0.23 in., elevation ??) while the other 7 contained one L symbol (height 0.3 in., width 0.12 in., elevation ??). Participants' encountered the stimuli in random order.

During the experiment, participants were seated at a table with a stimulus placed directly in front of them. Participants were asked to determine for each stimulus if it contained a target L, and if so to indicate its position. The participants used all 5 fingers on their dominant hands (only one blind participant was left handed), and started each trial with their index fingers placed in the center of the stimulus. A computer beep indicated when the trial had begun and the participant could begin searching.

The positions of the participants' index fingers were tracked by taping sensors (2.0 mm by 9.9 mm) to the tops of their nails. Wires from the sensors ran through a wrist band and then traveled up the far wall to avoid falling under participants' fingers. Fingers were tracked in three dimensions at originally 240 Hz with 1.4 mm root mean square position error using the 3D trakSTAR system (Northern Digital, Inc.). Trajectories were downsampled to 12 Hz to reduce computation time, which did not appreciably alter the trajectories' appearance. Each trial was temporally cropped to remove tracking data before the trial began (before the participant began moving) and after the trial ended (when the participant stopped moving or lifted his/her hand from the stimulus).

3) Analyses:

a) Specifying the Potential Function: A potential function associated with each stimulus was modeled as the sum from three sources: (1) distractors, (2) the target, and (3) a nonspecific general potential. The potential associated with each distractor was an Ornstein-Uhlenbeck (O-U) term, limited to be non-zero only when finger position was within 0.5 in. of the distractor's center. If the potential function traveled beyond the reach of a fingertip, it would imply that the participant had prior knowledge about stimulus layout and "felt" the attraction/repulsion of a distractor from anywhere on the stimulus. Similar to the distractors, the target was modeled using an O-U term that was zero beyond the 0.5 in. diameter around the target's center. Both the O-U term for distractors and target were allowed to vary in magnitude for x and y, and allowed to interact with whether the participant was blind or sighted. Finally, a high-order polynomial in x and y provided a general potential function for each stimulus. The potentials were fit using linear mixed effects models, with random effects of participant, trial (nested in participant), and index/time (nested in trial) using [16].

B. Results

In total there were 4 incorrect trials across the participants, and these were excluded from further analyses. Participants' average times (Table I) were shorter when the search target was present and shorter for blind participants, which is consistent with previous visual search [17] and haptics research [18], respectively. Given the low number of participants, no statistical tests were performed on trial times.

TABLE I: Participants' average trial times (with SEs).

Target	Sighted ($n = 3$)	Blind ($n = 3$)
Present	14.28 (1.79) sec	6.40 (1.24) sec
Absent	23.77 (2.68) sec	16.62 (4.20) sec

An example trajectory is shown in Fig. 1. In this example, the participant's index finger starts in approximately the center of the stimulus, and ends on the target L in the upper right. The participant also touches the two distractor T's in the lower left. However, in many trials the participant did not exhaustively explore all distractors before finding the target or declaring (correctly) that there was no target. Incorrect trials were not included in analyses.

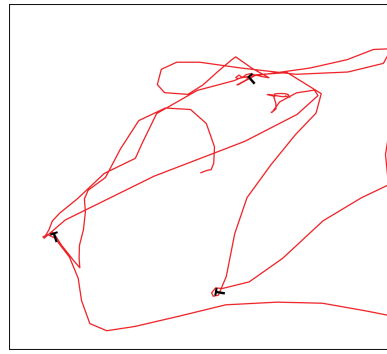

Fig. 1: Example trajectory (red) on stimulus (black).

1) Autocorrelation: The discretized Langevin equation, Eq. 9, is a second-order autoregressive (AR) model. The sample partial autocorrelation function (pACF) for an autoregressive model of order p, AR(p) is expected to have non-zero values for lags up to p, and then be zero for lags greater than p [19, 116]. A summary of the pACFs observed for all 80 trials, in x and y (which had no discernible differences) is shown in Fig. 2. Most notably, the first two lags have pACF values reliably significantly different from zero, consistent with an AR(2) process.

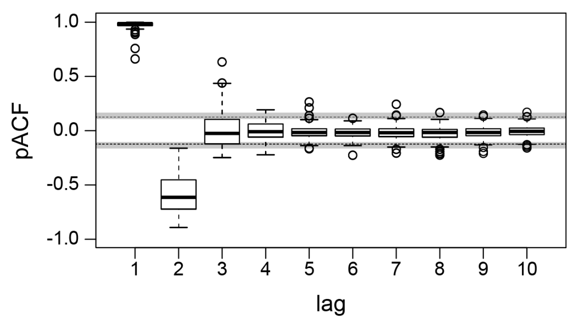

Fig. 2: Box and whisker plots summarizing the sample partial autocorrelation functions for all trials (80) and axes (x and y). Gray boxes with dashed lines show 25%, 50%, and 75% quantiles of Wald significance thresholds.

2) Potential Function Modeling: Model results for the potential function are shown in Table II. Both autoregressive terms were significant, consistent with the full Langevin Eq. 9, and not the Smoluchowski approximation Eq. 10. The significant intercept (Table II, Line 1) indicates some bias for fingers to move down and to the left, and the non-significant dummy variable for blind participants (Line 2) indicates that this bias is not significantly different for blind and sighted subjects. Allowing the bias to vary for x and y did not significantly improve the model based on the Bayesian Information Criterion (BIC): original BIC = 4197, allowing axis variation BIC = 4204.

TABLE II: Model terms, estimates (Est.), SEs, and p values. Terms $\mathbb{1}_c$ are 1 when the condition c is satisfied (participant is blind or r_{i-1} belongs to x or y axis), 0 otherwise.

Model Term	Est. $\times 10^{-3}$	SE $\times 10^{-3}$	p
1. (Intercept)	-120.12	(26.34)	< 0.001***
2. $\mathbb{1}_{\text{blind}}$	1.27	(5.09)	0.815
3. r_{i-1}	1623.31	(4.89)	< 0.001***
4. r_{i-2}	-624.94	(4.27)	< 0.001***
5. Targ. O-U$_{x-1}$	408.34	(112.20)	< 0.001***
6. Targ. O-U$_{x-1} \times \mathbb{1}_{\text{blind}}$	-233.18	(160.43)	0.146
7. Targ. O-U$_{y-1}$	369.05	(18.00)	< 0.001***
8. Targ. O-U$_{y-1} \times \mathbb{1}_{\text{blind}}$	103.38	(30.97)	< 0.001***
9. Dist. O-U$_{x-1}$	252.82	(7.69)	< 0.001***
10. Dist. O-U$_{x-1} \times \mathbb{1}_{\text{blind}}$	-77.35	(10.12)	< 0.001***
11. Dist. O-U$_{y-1}$	2.35	(0.94)	0.012*
12. Dist. O-U$_{y-1} \times \mathbb{1}_{\text{blind}}$	4.52	(1.05)	< 0.001***
13. $(-2x_{i-1}) \times \mathbb{1}_x$	5.18	(1.55)	< 0.001***
14. $(-3x_{i-1}^2) \times \mathbb{1}_x$	-0.10	(0.13)	0.418
15. $(-4x_{i-1}^3) \times \mathbb{1}_x$	0.16	(0.04)	< 0.001***
16. $(-3y_{i-1}^2) \times \mathbb{1}_y$	-0.65	(0.14)	< 0.001***
17. $(-4y_{i-1}^3) \times \mathbb{1}_y$	0.21	(0.04)	< 0.001***

$^{*}p < 0.05$, $^{**}p < 0.01$, $^{***}p < 0.001$

a) Target and Distractor O-U Processes: Both targets (Table II, Lines 5 and 7) and distractors (Lines 9 and 11) were estimated as O-U valleys ($\alpha > 0$), reflecting that they were "attractive" to participants' fingertip locations. Targets were overall more attractive than distractors. Targets were significantly more attractive (in y) for participants who were blind than for participants who were sighted (Line 8). In contrast, distractors were much less attractive (in y, and marginally more in x) for blind participants than sighted participants (Lines 10 and 12).

b) High-Order Polynomial: High-order polynomial terms (Table II, Lines 13-17) were included to capture any general potential function associated with all stimuli. Including up to fourth-order terms produced the best model as indicated by having the lowest BIC when compared to other models with varying number of polynomial terms: 2$^{\text{nd}}$ order BIC = 4213, 3$^{\text{rd}}$ order BIC = 4211, 4$^{\text{th}}$ order BIC = 4197, 5$^{\text{th}}$ order BIC = 4216, and 6$^{\text{th}}$ order BIC = 4230.

Note that some low-order terms were dropped from the model to avoid singularity (Table II). However, this was not a concern because the interpretation of the polynomials comes from their overall shape (Sec. II-C), shown in Fig. 3. Upwards inflection towards stimulus edges acts to keep finger positions within the stimulus.

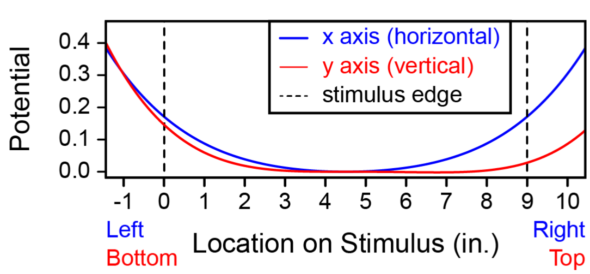

Fig. 3: Potential function fit by high-order polynomial terms. Only significantly non-zero terms shown.

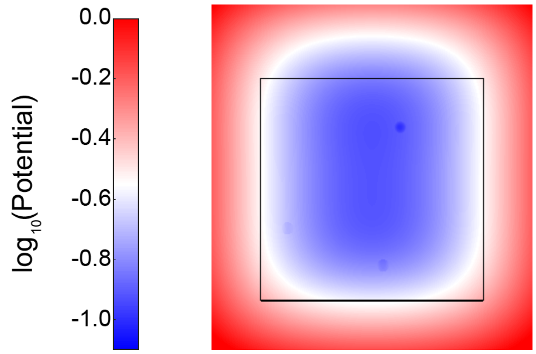

(a) Estimated potential. Black box outlines stimulus edges.

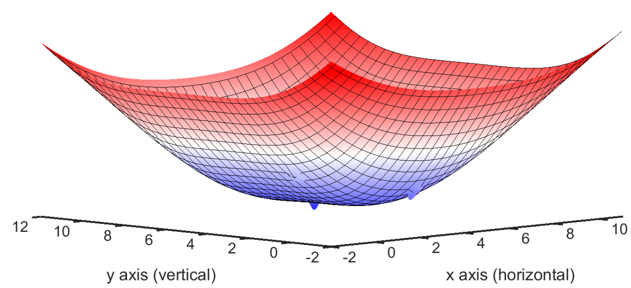

(b) Estimated potential as a surface. Location on stimulus is shown in in., with (0,0) being the bottom-left corner of the stimulus. White band is located approximately on stimulus edges (see Fig. 4a).

Fig. 4: Example potential function for a sighted participant based on model results (Table II) and stimulus in Fig. 4.

c) Complete Potential Function: A complete potential function for a stimulus is the sum of potentials from the target, distractors, and polynomial terms. An example potential function is shown in Fig. 4. The general shape of the potential function keeps finger positions within the stimulus. Three local low-potential O-U valleys are associated with the single Target (stimulus upper right) and two distractors (lower left). These are visible in Fig. 4a as three circular dark areas, and in Fig. 4b as three stalactites hanging from the bottom of the potential surface.

3) Simulation: Trajectories can be simulated using Eqs. 12 and 12 and model results (Table II). A simulation on the stimulus in Fig. 1 is shown in Fig. 5.

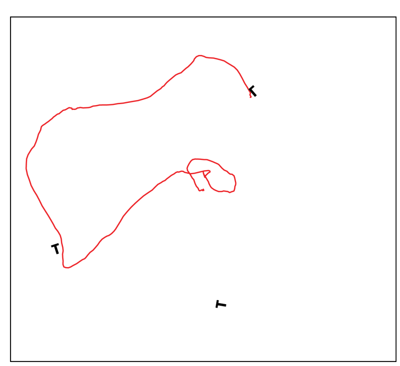

Fig. 5: Simulated trajectory (red) on stimulus (black).

IV. DISCUSSION

This paper covers the SDE framework to describe, compare, and predict finger-movement trajectories. Using this approach, differences in trajectories between experimental groups can be statistically compared. In the current example, a significant difference was found between how blind and sighted participants interacted with distractors and targets. Specifically, they are more focused on the target, and less focused on distractors, compared to sighted participants.

SDEs can also be used to simulate finger-movement trajectories. While the example provided in Fig. 5 uses a stimulus that was used in modeling, it should be obvious that simulation can also be conducted on stimuli that were not used for collecting data included in the SDE model. If simulation is the primary scientific purpose of a study, it may be desirable to use some data for model training and some for testing, with non-overlapping stimuli.

Modeling finger-movements using SDEs was derived using the analogy between fingertip position and a Brownian particle. The result was a regression model for finger-movement trajectories, where model effects were provided through a potential function and random movements/errors were conceptualized as Brownian perturbances. However, the resulting model should not be taken too seriously, as it does *not* specify the mechanism through which finger movements arise. This is similar to any other model in the behavioral sciences, e.g., one relating income and education level. While the model describes the relationship between variables, it does not capture the mechanism of this relationship. In contrast to a physics model, in the behavioral sciences "all models are wrong, some models are useful" [20].

The current model can be extended in several ways. While the current work describes two-dimensional (2D) data, it is self-evident how to extend the SDE approach to three-dimensional (3D) data. Beyond this, the current illustrative example uses thresholding to keep the effect of stimulus features on the movement trajectories local. An alternative approach could make use of hidden Markov state space models, in which the participants are assumed to have hidden behavioral states, such as examination of a distractor or general exploration. Being in a behavioral state would be probabilistic, and could depend on the proximity of the participant's finger(s) to stimulus features, exploration history/time, and could explicitly model noise associated with the finger-tracking method. These types of models are used to describe animal movements [21], [22] without a potential function, to describe switching between high- and low-variance random walks. Extending the potential function approach to a hidden Markov state space model could provide an alternative to the scheme used here, and may provide different insights into finger-movement strategies.

ACKNOWLEDGMENT

We thank Daisy Lei for help with data collection and processing, and Joel Corbo and Jed Duersch for feedback.

REFERENCES

[1] D. R. Brillinger, H. Preisler, A. Ager, and M. Wisdom, "Stochastic differential equations in the analysis of wildlife motion," *2004 Proceedings of the American Statistical Association, Statistics and the Environment Section*, 2004.

[2] H. K. Preisler, A. A. Ager, B. K. Johnson, and J. G. Kie, "Modeling animal movements using stochastic differential equations," *Environmetrics*, vol. 15, no. 7, pp. 643–657, 2004.

[3] D. R. Brillinger, H. K. Preisler, A. A. Ager, and J. G. Kie, "The use of potential functions in modelling animal movement," in *Data Analysis from Statistical Foundations*, A. K. M. E. Saleh, Ed. Huntington, NY: Nova Science, 2001, pp. 369–386.

[4] A. Einstein, "On the movement of small particles suspended in a stationary liquid demanded by the molecular-kinetic theory of heat," in *Investigations on the theory of the Brownian movement*, R. Fürth, Ed. New York: Dover, 1905/1956, pp. 1–18.

[5] W. Coffey, Y. P. Kalmykov, and J. T. Waldron, *The Langevin equation: With applications to stochastic problems in physics, chemistry, and electrical engineering*. River Edge, NJ: World Scientific, 2004, vol. 14.

[6] D. S. Lemons and A. Gythiel, "Paul Langevin's 1908 paper 'On the Theory of Brownian Motion'['Sur la théorie du mouvement Brownien,' CR Acad. Sci. (Paris) 146, 530–533 (1908)]," *American Journal of Physics*, vol. 65, no. 11, pp. 1079–1081, 1997.

[7] E. Nelson, *Dynamical theories of Brownian motion*. Princeton, NJ: Princeton University Press, 1967.

[8] S. M. Iacus, *Simulation and inference for stochastic differential equations: with R examples*. New York: Springer, 2008.

[9] S. Chandrasekhar, "Stochastic problems in physics and astronomy," *Reviews of Modern Physics*, vol. 15, no. 1, p. 1, 1943.

[10] M. W. Hirsch, S. Smale, and R. L. Devaney, *Differential equations, dynamical systems, and an introduction to chaos*. Amsterdam: Elsevier/Academic Press, 2004, vol. 60.

[11] D. R. Brillinger, B. Stewart, and C. Littnan, "Three months journeying of a Hawaiian monk seal," *IMS Collections*, vol. 2, pp. 246–264, 2006.

[12] H. K. Preisler, A. A. Ager, and M. J. Wisdom, "Analyzing animal movement patterns using potential functions," *Ecosphere*, vol. 4, no. 3, p. 32, 2013.

[13] D. R. Brillinger, H. K. Preisler, A. A. Ager, and J. G. Kie, "An exploratory data analysis (EDA) of the paths of moving animals," *Journal of Statistical Planning and Inference*, vol. 122, no. 1, pp. 43–63, 2004.

[14] E. E. Holmes, "Are diffusion models too simple? a comparison with telegraph models of invasion," *American Naturalist*, pp. 779–795, 1993.

[15] E. A. Codling, M. J. Plank, and S. Benhamou, "Random walk models in biology," *Journal of the Royal Society Interface*, vol. 5, no. 25, pp. 813–834, 2008.

[16] J. Pinheiro, D. Bates, S. DebRoy, D. Sarkar, and R Core Team, *nlme: Linear and Nonlinear Mixed Effects Models*, 2014, r package version 3.1-117. [Online]. Available: http://CRAN.R-project.org/package=nlme

[17] M. M. Chun and J. M. Wolfe, "Just say no: How are visual searches terminated when there is no target present?" *Cognitive Psychology*, vol. 30, no. 1, pp. 39–78, 1996.

[18] V. Morash, A. E. Connell Pensky, S. T. W. Tseng, and J. A. Miele, "Effects of using multiple hands and fingers on haptic performance in individuals who are blind," *Perception*, vol. 43, no. 7, pp. 569–588, 2013.

[19] J. D. Cryer and K.-S. Chan, *Time series analysis with applications in R*, 2nd ed. New York, NY: Springer, 2008.

[20] G. E. Box, W. G. Hunter, and J. S. Hunter, "Statistics for experimenters," 1978.

[21] M. A. Silva, I. Jonsen, D. J. Russell, R. Prieto, D. Thompson, and M. F. Baumgartner, "Assessing performance of bayesian state-space models fit to argos satellite telemetry locations processed with Kalman filtering," *PloS One*, vol. 9, no. 3, p. e92277, 2014.

[22] I. Jonsen, M. Basson, S. Bestley, M. Bravington, T. Patterson, M. W. Pedersen, R. Thomson, U. H. Thygesen, and S. Wotherspoon, "State-space models for bio-loggers: A methodological road map," *Deep Sea Research Part II: Topical Studies in Oceanography*, vol. 88, pp. 34–46, 2013.